

1 **The ADP-glucose pyrophosphorylase from *Melainobacteria*: a comparative**
2 **study between photosynthetic and non-photosynthetic bacterial sources**

3
4 María V. Ferretti^a, Rania A. Hussien^{b,c}, Miguel A. Ballicora^b,

5 Alberto A. Iglesias^a, Carlos M. Figueroa^a, Matías D. Asencion Diez^{a§}

6
7 ^aInstituto de Agrobiotecnología del Litoral, Universidad Nacional del Litoral, Consejo
8 Nacional de Investigaciones Científicas y Técnicas, Facultad de Bioquímica y Ciencias
9 Biológicas, Santa Fe, Argentina

10 ^bDepartment of Chemistry and Biochemistry, Loyola University Chicago, Chicago, Illinois, USA

11 ^cDepartment of Chemistry, Al Baha University, P.O. Box 1988. Al Baha, Saudi Arabia Imam
12 Mohammed Ibn Saud Islamic University, Riyadh, Saudi Arabia

13
14
15 [§]**Corresponding author:**

16 Dr. Matías D. Asencion Diez masencion@fcb.unl.edu.ar

17 Instituto de Agrobiotecnología del Litoral (UNL-CONICET). CCT-Santa Fe, Colectora
18 Ruta Nac 168 km 0. Santa Fe (3000), Argentina.

20 **Abstract**

21 Until recently, all members of the cyanobacterial phylum were considered capable of
22 performing oxygenic photosynthesis. This view has been questioned after the discovery of
23 a group of presumed non-photosynthetic cyanobacteria named *Melainabacteria*. Using
24 metagenomic data, we identified sequences encoding putative ADP-glucose
25 pyrophosphorylase (EC 2.7.7.27, ADP-GlcPPase) from free-living and intestinal
26 *Melainabacteria*. These genes were *de novo* synthesized and overexpressed in *Escherichia*
27 *coli*. The purified recombinant proteins from the free-living and the intestinal
28 *Melainabacteria* showed ADP-GlcPPase activity, with V_{\max} values of 2.3 and 7.1 U/mg,
29 respectively. Both enzymes had similar affinities towards ATP ($S_{0.5} \sim 0.3$ mM) although the
30 one from the intestinal source displayed a 6-fold higher affinity for glucose-1P. Both
31 recombinant ADP-GlcPPases were sensitive to allosteric activation by glucose-6P ($A_{0.5}$
32 ~ 0.3 mM), and to inhibition by Pi and ADP ($I_{0.5}$ between 0.2 to 3 mM). Interestingly, the
33 enzymes from *Melainabacteria* were insensitive to 3-phosphoglycerate, which is the
34 principal activator of ADP-GlcPPases from photosynthetic cyanobacteria. To the best of
35 our knowledge, this is the first biochemical characterization of an active enzyme from
36 *Melainabacteria*, offering further data to discussions regarding their phylogenetic position.
37 This work contributes to a better understanding regarding the evolution of allosteric
38 mechanisms in ADP-GlcPPases, an essential enzyme for the synthesis of glycogen in
39 prokaryotes and starch in plants.

40

41 **Introduction**

42 Most living organisms produce α -1,4-glucans as a strategy to store carbon and
43 energy, which can be mobilized under conditions of nutrient deficiency. Bacteria and
44 heterotrophic eukaryotes accumulate glycogen, whereas starch is the reserve carbohydrate
45 in green algae and higher plants [1]. The build-up of glycogen and starch in bacteria and
46 plants, respectively, involves a similar pathway where ADP-glucose (ADP-Glc) is the
47 glycosyl donor for polysaccharide elongation. In such metabolic route, the sugar nucleotide
48 synthesis is the rate-limiting step, catalyzed by ADP-Glc pyrophosphorylase (ADP-
49 GlcPPase, EC 2.7.7.27). Indeed, ADP-GlcPPase is allosterically regulated by metabolites
50 from the central carbon utilization pathway in the respective organism [1–4]. In this
51 context, the enzyme from *Escherichia coli* is mainly activated by fructose-1,6-
52 biphosphate, a key intermediate in the Embden-Meyerhof route. At the same time,
53 fructose-6-phosphate (Fru-6P) and pyruvate are the principal activators of the enzyme from
54 *Agrobacterium tumefaciens*, where the Entner-Doudoroff is the main glycolytic pathway
55 [5–9]. Similarly, ADP-GlcPPases from organisms performing oxygenic photosynthesis
56 (cyanobacteria, green algae, and higher plants) are primarily activated by 3-
57 phosphoglycerate (3-PGA) and inhibited by inorganic orthophosphate (Pi) [1,10–12].

58 Cyanobacteria are a highly diverse group of Gram-negative prokaryotes that
59 colonized a wide range of environments, from desert crusts to fresh and marine waters and
60 from the tropics to the poles [13]. These microorganisms modified the Earth's atmosphere
61 through oxygenic photosynthesis, which enabled the evolution of life into more complex
62 forms [14]. Photosynthetic cyanobacteria have been studied for decades, and their diversity
63 is described in terms of both morphology and genetics [15–17]. With the development of

64 metagenomics, an unexpected variety of organisms was unveiled in many ecosystems,
65 including non-photosynthetic bacteria closely related to the clade Cyanobacteria [18–21].

66 One group of these microorganisms was named *Melainabacteria* [19] because several
67 representatives of this cluster were found in aphotic environments. Firstly, they were
68 considered as a sister phylum of Cyanobacteria [19]; later, data from genomic sequences
69 analysis suggested that *Melainabacteria* belongs to the superphylum of Cyanobacteria [20],
70 although these suggestions have not been validated so far. Based on this evidence, a new
71 classification has been proposed for the phylum Cyanobacteria. This arrangement includes
72 the class-level lineages *Oxyphotobacteria* (cyanobacteria performing oxygenic
73 photosynthesis) and *Melainabacteria*, as well as a third class called ML635J-21 [20],
74 recently named *Sericytochromatia* [22]. After diverging from *Melainabacteria*, the
75 *Oxyphotobacteria* developed oxygenic photosynthesis around 2.4–2.35 billion years ago, as
76 estimated from the molecular clock and geological data [22–24].

77 *Melainabacteria*, described for the first time only a few years ago, is a group of
78 poorly characterized anaerobic bacteria. To date, only a handful of *Melainabacteria*
79 genomes have been sequenced [22], and thus, the metabolism, biological functions, and
80 ecological roles of these organisms are not fully known. Representatives of
81 *Melainabacteria* have been found in photic and aphotic environments such as (i) sub-
82 surface groundwater [19], (ii) lake water and algal biofilms [22,25], (iii) marine and
83 lacustrine sediment [26], and (iv) animal and human faeces [20] and guts [26]. All
84 sequenced genomes of *Melainabacteria* confirm they lack the entire photosynthetic
85 apparatus, which may support the hypothesis that acquisition of photosystems in
86 *Oxyphotobacteria* occurred after divergence from the non-photosynthetic *Melainabacteria*

87 [20,22]. Consequently, the characterization of enzymes from main metabolic segments
88 (such as the synthesis of the energy/carbon storage molecule glycogen) is critical to sum
89 biochemical criteria to help the scientific community to further classify this group of
90 bacteria.

91 By studying the biochemical properties of cyanobacterial ADP-GlcPPases, an
92 evolutionary thread could be established between bacterial glycogen and starch synthesis
93 metabolism [1,2,27,28]. Hence, the particular regulatory properties of ADP-GlcPPases
94 prompted us to explore the features of this enzyme in *Melainabacteria*. In this framework,
95 we *de novo* synthesized the genes encoding ADP-GlcPPases from intestinal (*inMelGlgC*)
96 and free-living (*flMelGlgC*) *Melainabacteria*. The recombinant proteins were produced,
97 purified, and kinetically characterized. For the sake of comparison, we also made the
98 homologous enzyme from photosynthetic *Anabaena* PCC 7120 (*AnaGlgC*). Our results
99 indicate that *Melainabacteria* ADP-GlcPPases have distinctive kinetic and regulatory
100 properties, which might fit a heterotrophic metabolism commonly found in diverse bacterial
101 organisms.

102

103 **Material and Methods**

104 *Chemicals, bacterial strains and plasmids*

105 Chemicals used for enzymatic assays were from Sigma-Aldrich (St. Louis, MO,
106 USA). All the other reagents were of the highest quality available. *Escherichia coli* Top 10
107 (Invitrogen) were used for plasmid maintenance. The *glgC* genes from *Anabaena* PCC
108 7120, intestinal and free-living *Melainabacteria* were expressed in *E. coli* BL21 (DE3)
109 (Invitrogen) using the pET28b vector (Novagen). DNA manipulations, molecular biology
110 techniques, and *E. coli* cultivation and transformation were performed according to
111 standard protocols [29].

112 *Phylogenetic analysis*

113 Amino acid sequences of ADP-GlcPPases from different organisms were
114 downloaded from the NCBI database (<http://www.ncbi.nlm.nih.gov>) and classified into
115 different groups using taxonomic data provided by the NCBI. Sequences were manually
116 curated to remove duplicates and near-duplicates (i.e., mutants and strains from the same
117 species). We constructed a preliminary alignment using the ClustalW multiple sequence
118 alignment server [30], which was then manually refined with the BioEdit 7.0 program [31].
119 Tree reconstruction was performed using the neighbour-joining algorithm with a bootstrap
120 of 1,000 in the program SeaView 4.3 [32]. The phylogenetic tree was prepared with the
121 FigTree 1.3 program (<http://tree.bio.ed.ac.uk/software/figtree/>).

122 *Cloning of glgC genes*

123 Genes encoding ADP-GlcPPases from intestinal and free-living *Melainabacteria*
124 were *de novo* synthesized (Bio Basic, Canada) according to genomic information for these

125 bacteria [19,21], available in the NCBI database (Nucleotide IDs CP017245.1 and
126 MFRL000000000.1, respectively). The genes encoding intestinal and free-living
127 *Melainabacteria* GlgC proteins (NCBI Protein IDs AOR37842.1 and OGI00355.1,
128 respectively) were optimized for expression in *E. coli* and inserted into the pET28b vector
129 between the *NdeI* and *SacI* restriction sites, to produce the recombinant proteins with an N-
130 terminal His-tag. The same procedure was performed for the gene encoding the *Anabaena*
131 PCC 7120 GlgC protein (NCBI Protein ID WP_010998776.1).

132 *Enzyme production and purification*

133 Transformed *E. coli* BL21 (DE3) were grown in YT2X medium (16 g/l tryptone; 10
134 g/l yeast extract; 5 g/l NaCl) supplemented with kanamycin (50 µg/ml) at 37 °C and 200
135 rpm, until reaching an optical density at 600 nm of ~0.6. Recombinant protein expression
136 was induced with 0.1 mM isopropyl-β-D-1-thiogalactopyranoside for 16 h at 18 °C. Cells
137 were harvested by centrifugation at 5000 × *g* for 10 min and stored at -20 °C until use.

138 His-tagged proteins were purified at 4 °C by immobilized metal affinity
139 chromatography (IMAC). Cells were resuspended in *Buffer H* [50 mM Tris-HCl pH 8.0,
140 300 mM NaCl, 10mM imidazole, 5% (v/v) glycerol] and disrupted by sonication. The
141 suspension was centrifuged twice at 30000 × *g* for 10 min, and the supernatant (crude
142 extract) loaded on a 1-ml His-Trap column (GE Healthcare) previously equilibrated with
143 *Buffer H*. The recombinant proteins were eluted with a linear gradient from 10 to 300 mM
144 imidazole in *Buffer H*. Fractions containing the highest activity were pooled, concentrated
145 to 2 ml, and dialyzed against *Buffer S* [50 mM HEPES-NaOH, 10% (w/v) sucrose, 0.2 mM
146 DTT, 1 mM EDTA]. The resulting enzyme samples preparations were stored at -80 °C until
147 use, remaining fully active for at least 10 months.

148 *Protein methods*

149 Protein concentration was determined with the Bradford reagent [33], using bovine
150 serum albumin (BSA) as a standard. The purity of the recombinant proteins was assessed
151 by sodium dodecyl sulfate-polyacrylamide gel electrophoresis (SDS-PAGE), according to
152 Laemmli [34]. Gels were loaded with 5 to 50 μ g of protein per well and stained with
153 Coomassie Brilliant Blue.

154 *Native molecular mass determination*

155 The native molecular mass of the recombinant proteins was determined by gel
156 filtration using a Superdex 200 10/300 column (GE Healthcare), previously calibrated with
157 protein standards (GE Healthcare), including thyroglobulin (669 kDa), ferritin (440 kDa),
158 aldolase (158 kDa), conalbumin (75 kDa), and ovalbumin (44 kDa). The void volume of
159 the column was determined using Dextran Blue (Promega).

160 *Enzyme activity assays*

161 ADP-GlcPPase activity was determined at 37 °C in the direction of ADP-Glc
162 synthesis, following the formation of P_i after hydrolysis of PP_i by inorganic
163 pyrophosphatase, using a highly sensitive colorimetric method [35]. Reaction mixtures
164 contained (unless otherwise specified) 50 mM MOPS-NaOH pH 8.0, 10 mM $MgCl_2$, 1.5
165 mM ATP, 0.2 mg/ml BSA, 0.5 U/ml yeast inorganic pyrophosphatase and a proper enzyme
166 dilution. Assays were initiated by the addition of 1.5 mM Glc-1P in a total volume of 50 μ l.
167 Reaction mixtures were incubated for 10 min at 37 °C and terminated by adding 400 μ l of
168 the Malachite Green reagent. The complex formed with the released P_i was measured at
169 630 nm in a 96-well microplate reader (Multiskan GO, Thermo).

170 To test P_i inhibition, ADP-GlcPPase activity was measured using a coupled-enzyme
171 spectrophotometric assay. Reaction mixtures contained 50 mM MOPS-NaOH pH 8.0, 10
172 mM $MgCl_2$, 0.3 mM phosphoenolpyruvate, 0.3 mM NADH, 2 mM ATP, 1 mg/ml rabbit
173 muscle glycogen, 0.8 U/ μ l *E. coli* glycogen synthase, 0.1 U/ μ l pyruvate kinase, 0.02 U/ μ l
174 lactate dehydrogenase, 0.2 mg/ml BSA and enzyme in a total volume of 50 μ l. The reaction
175 was initiated with 2 mM Glc-1P, and activity was measured by following NADH oxidation
176 at 340 nm and 37 °C using a 384-microplate reader (Multiskan GO, Thermo). One unit of
177 activity (U) is defined as the amount of enzyme catalyzing the formation of 1 μ mol of
178 product per min, under the above specified conditions.

179 Saturation curves were constructed by assaying enzyme activity at different
180 concentrations of the variable substrate or effector, while the others remained at saturating
181 levels. Plots of enzyme activity (U/mg) *versus* substrate (or effector) concentration (mM)
182 were used to calculate the kinetic constants, by fitting the experimental data to a modified
183 Hill equation [36]. Fitting was performed with the Levenberg-Marquardt non-linear least-
184 squares algorithm provided by the computer program Origin 8.0 (OriginLab). Accordingly,
185 we calculated the Hill coefficient (n_H), the maximal velocity (V_{max}), and the concentrations
186 of activator, substrate or inhibitor giving 50% of the maximal activation ($A_{0.5}$), velocity
187 ($S_{0.5}$) or inhibition ($I_{0.5}$), respectively. All kinetic constants are the mean of at least three
188 independent sets of data, which were reproducible within a range of \pm 10%.

189 **Results**

190 *Identification of glgC genes, molecular cloning, and phylogenetic analysis of ADP-*
191 *GlcPPases from Melainabacteria*

192 We identified *glgC* genes, encoding putative ADP-GlcPPases, in metagenomic
193 databases from intestinal (*inMelglgC*) and free-living (*flMelglgC*) *Melainabacteria* [19,21].
194 The *inMelglgC* (1,236 bp) and *flMelglgC* (1,233 bp) genes code for proteins of ~45 kDa,
195 which share identities of 66.18% between them; ~35% with *Anabaena* GlgC; ~43% with
196 the *A. tumefaciens* GlgC; and ~44% with the *S. coelicolor* GlgC. Further to this
197 comparison, it is worth considering the already established structure to function
198 relationships between ADP-GlcPPases regarding central metabolism in one organism [1,2].
199 In this context, we extended the comparison of the GlgCs' amino acid sequences, obtaining
200 the phylogenetic tree shown in Figure 1. As shown, the analysis protein found GlgCs from
201 *Melainabacteria* in a cluster separated from those present in bacteria performing oxygenic
202 photosynthesis. Indeed, *Melainabacteria* ADP-GlcPPases locate closer to proteins from
203 heterotrophic bacteria, particularly Actinobacteria. These results trigger additional
204 biological and evolutionary questions since the taxonomic classification of *Melainabacteria*
205 [20], and the phylogenetic position of their ADP-GlcPPases are markedly different (Figure
206 1).

207 To explore beyond the phylogenetic relationships between ADP-GlcPPases, we *de*
208 *novo* synthesized the genes *inMelglgC* and *flMelglgC* to produce and characterize the
209 respective recombinant proteins. For comparison, we followed the same approach to obtain
210 the enzyme from *Anabaena* PCC 7120, which was already characterized in detail [11].

211 Supplemental Figure 1A illustrates that the ADP-GlcPPases from both *Melainabacteria*
212 (in*Mel*GlgC and fl*Mel*GlgC), as well as that from *Anabaena* PCC 7120 (*Ana*GlgC), were
213 obtained with a high purity level. The purified enzymes exhibited specific activity values of
214 7.1 (in*Mel*GlgC), 2.3 (fl*Mel*GlgC), and 0.31 (*Ana*GlgC) U/mg (in the absence of allosteric
215 activators). Both ADP-GlcPPases from *Melainabacteria* eluted from the gel filtration
216 column with molecular masses between 180 and 190 kDa (Supplemental Figure 1B).
217 Considering the theoretical mass of these proteins and results obtained by SDS-PAGE
218 (Supplemental Figure 1A), we conclude that both enzymes are homotetramers, which
219 agrees with the quaternary structure of ADP-GlcPPases characterized so far [1,2].

220 *Kinetic and regulatory properties of Melainabacteria ADP-GlcPPases*

221 The recombinant ADP-GlcPPases were kinetically characterized in the direction of
222 ADP-Glc synthesis. Saturation curves for Glc-1P and ATP of the *Melainabacteria* enzymes
223 showed deviation from the hyperbolic behavior (Supplemental Figure S2), with similar
224 affinities towards ATP in both cases (Table 1). However, in*Mel*GlgC displayed a 6-fold
225 lower $S_{0.5}$ for Glc-1P than fl*Mel*GlgC (Table 1). In the comparative analysis, *Ana*GlgC
226 exhibited an apparent affinity for Glc-1P one order of magnitude higher than fl*Mel*GlgC
227 (Table 1). We also explored the effect of different metabolites, known to activate or inhibit
228 ADP-GlcPPases from various organisms [1,2,9,37–39], on the activity of the
229 *Melainabacteria* enzymes. As detailed in Figure 2, many of the assayed compounds exerted
230 changes on the kinetics of in*Mel*GlgC and fl*Mel*GlgC. Among these, glucose-6P (Glc-6P),
231 Fru-6P, and mannose-6P (Man-6P) activated, while ADP and Pi inhibited both enzymes
232 (Figure 2). Noteworthy, the activity of *Melainabacteria* enzymes did not significantly
233 change in the presence of 3-PGA (Figure 2), the primary activator of ADP-GlcPPases from

234 oxygenic photosynthetic organisms [1,2,11], including those from cyanobacterial sources
235 characterized so far [28,40,41].

236 We then performed a detailed study of the activation kinetics for the different ADP-
237 GlcPPases studied in this work. As shown in Figure 3A, Glc-6P activated in*Mel*GlcC and
238 fl*Mel*GlcC 54- and 12-fold, respectively, with similar $A_{0.5}$ values (Supplemental Table S1).
239 The activation of *Ana*GlcC by Glc-6P reached a maximum of 5-fold, and the relative
240 affinity towards the hexose-P was 5-fold lower compared to the enzymes from
241 *Melainabacteria* (Supplemental Table S1). Further analysis of substrate saturation kinetics
242 showed that Glc-6P did not significantly alter the apparent affinities of the enzymes
243 towards ATP. Instead, Glc-6P increased 1.6- and 3.8-fold the Glc-1P apparent affinities of
244 in*Mel*GlcC and fl*Mel*GlcC, respectively; conversely, Glc-6P decreased 10-fold the Glc-1P
245 apparent affinity in the case of *Ana*GlcC (Table 1). Fru-6P and Man-6P (respectively)
246 activated in*Mel*GlcC (40- and 15-fold), fl*Mel*GlcC (4- and 13-fold), and *Ana*GlcC (15- and
247 6-fold), with $A_{0.5}$ values in the range 0.5-1.5 mM (Supplemental Table S1). Figure 3B
248 shows that 3-PGA has no effect on the activity of ADP-GlcPPases from *Melainabacteria*
249 (up to 5 mM). At the same time, *Ana*GlcC was activated 30-fold (with an $A_{0.5}$ of 0.2 mM),
250 which agrees with previous work [11]. Inhibition kinetics confirmed that ADP and Pi are
251 inhibitors of the studied enzymes (Supplemental Table S2), although Pi inhibition was
252 more pronounced in *Ana*GlcC than in in*Mel*GlcC and fl*Mel*GlcC ($I_{0.5}$ values were 0.09,
253 0.23, and 2.3 mM, respectively).

254 **Discussion**

255 It was initially thought that all members of the cyanobacterial phylum were capable
256 of performing oxygenic photosynthesis [20,42]. This scenario was recently questioned after
257 discovering *Melainabacteria*, a bacterial group closely related to Cyanobacteria at a
258 phylogenetic level but incapable of performing photosynthesis [19,21]. The analysis of
259 metagenomic information allowed us to find genes from *Melainabacteria* related to
260 carbohydrate metabolism, particularly glycogen synthesis (see below and Table 2). Then,
261 analyzing the kinetic and regulatory properties of key metabolic enzymes would contribute
262 to the biochemical and evolutionary discussion concerning the classification of
263 cyanobacteria and their sister-clades, such as *Melainabacteria*.

264 We focused on sequences encoding ADP-GlcPPase, which catalyzes the first
265 committed step in the pathway for bacterial glycogen synthesis [2,4]. As previously
266 mentioned, ADP-GlcPPases from Cyanobacteria performing oxygenic photosynthesis are
267 activated by 3-PGA, while glycolytic intermediates control those from heterotrophic
268 microorganisms, *e.g.*, fructose-1,6-bisphosphate and pyruvate in the enzyme from *E. coli*
269 [5–9]. Here, it is important to remark that ADP-GlcPPase’s regulatory properties are
270 intimately related to main metabolic pathways in the organisms, then constituting a relevant
271 issue to inferring on *Melainabacteria* metabolism. The comparative analysis of the
272 structural, kinetic, and regulatory properties of different ADP-GlcPPases has contributed to
273 understanding better the evolution of allosteric mechanisms in this family of biological
274 catalysts [8,9,43–46]. In this regard, we sought to characterize ADP-GlcPPases from
275 *Melainabacteria* since these bacteria seem to be located at a phylogenetic enclave which
276 deserves further characterization. Hence, we constructed a phylogenetic tree to gain more

277 information concerning the evolutionary relationship between *Melainabacteria* ADP-
278 GlcPPases and enzymes from other taxonomic groups. Our phylogenetic analysis showed
279 that *Melainabacteria* sequences were grouped closer to heterotrophic bacteria than to
280 photosynthetic Cyanobacteria (Figure 1). ADP-GlcPPases from different prokaryotic
281 sources showed to be homotetrameric, with subunits of about 45–50 kDa [2]. So far, the
282 only exception is the enzyme from Firmicutes, a heterotetramer composed of two subunit
283 types, GlgC and GlgD [2,47,48]. We could only find a single *glgC* gene in metagenomic
284 data from *Melainabacteria* and, after recombinant expression of two different enzymes; we
285 proved that both proteins are homotetramers (Supplemental Figure 1). Thus, ADP-
286 GlcPPases from this Cyanobacteria sister-clade have a structural architecture similar to that
287 from photosynthetic cyanobacteria (and most bacterial sources but Firmicutes), sustaining
288 the importance of advancing with the kinetic and regulatory characterization of these
289 enzymes to elucidate their structure-to-function relationships.

290 In a general view, the enzymes from *Melainabacteria* presented specific activities
291 one order of magnitude higher than that from *Anabaena* PCC 7120 (in the absence of
292 allosteric activators). However, the latter showed a higher apparent affinity towards ATP
293 and Glc-1P (Table 1). Noteworthy, the catalytic capacity of ADP-GlcPPases from
294 *Melainabacteria* was similar to that observed for enzymes from heterotrophic bacteria
295 [1,2,49]. Interestingly, ADP-GlcPPases from *Melainabacteria* lack 3-PGA activation but
296 are highly sensitive to hexose-6P (Glc-6P, Fru-6P, and Man-6P; Supplemental Table S1),
297 similarly to the enzymes from heterotrophic bacteria [2], particularly those from
298 Actinobacteria [37,39,50,51]. Remarkably, actinobacterial ADP-GlcPPases and those from
299 *Melainabacteria* are located in the same branch of the phylogenetic tree (Figure 1). The

300 activation by Glc-6P of in*Mel*GlgC (Figure 3) is the highest reported so far for this
301 metabolite, while the effect on fl*Mel*GlgC is similar to that from the *Rhodococcus jostii*
302 enzyme [50]. Given the proximity between ADP-GlcPPases from Actinobacteria and
303 *Melainabacteria*, we foresee that these enzymes will be useful to explain the molecular
304 mechanism underlying ADP-GlcPPase activation by Glc-6P. Even more, since Glc-6P is
305 the common effector between ADP-GlcPPases from photosynthetic and some heterotrophic
306 organisms (Figure 3 and Table 1), elucidating this allosteric mechanism will be critical to
307 illuminate the evolutionary scenario related to changes on the sensitivity to a given effector.

308 Using the available metagenomic data, we also analyzed the existence in
309 *Melainabacteria* of other genes related to glycogen metabolism in bacteria. As shown in
310 Table 2, we found these organisms contain *glgA* and *glgB* genes, putatively encoding
311 glycogen synthase (EC 2.4.1.21) and branching enzyme (EC 2.4.1.18). Curiously, the
312 putative GlgA from *Melainabacteria* (so far, the only one) displays higher identity to the
313 two homologous enzymes from *Synechocystis* PCC 6803, GlgA1 (37%) and GlgA2 (33%) -
314 the latter probably related to glucan priming in some Cyanobacteria [52]- than to the one
315 from *E. coli* (~29%) or *Mycobacterium tuberculosis* (~21%), recently renamed GlgM [53].
316 Besides, the GlgAs from *Melainabacteria* and *Anabaena* share a 36% identity between
317 each other. Also, the *Anabaena* GlgA possess 73% and 30% identity with the GlgA1 and
318 GlgA2 proteins from *Synechocystis*, respectively. Regarding the branching enzyme (GlgB),
319 we found a protein sequence in *Melainabacteria* with a 39% identity with the branching
320 enzyme from *Thermus thermophilus*, which is the only GlgB belonging to the GH57 family
321 in CAZy [54] for which both kinetic and structural data are available [55]. Curiously, the
322 putative GlgB from *Melainabacteria* showed 93% identity with a putative homologous

323 enzyme from *Clostridium* (see supplemental Figure S3), but only 30 and 40% identity with
324 GH57 GlgBs from *Bacillus halodurans* and *Thermococcus kodakarensis*, respectively. On
325 the other hand, when the GlgB from *Anabaena* (belonging to the CAZy GH13 family, as
326 most of the GlgBs already characterized) was used as a template, no significant
327 coincidences were found in the *Melainabacteria* genomic information. Recently, it was
328 suggested that the GH57 GlgB produces glucans with short branches, although remaining
329 work should be completed to understand the precise role of this type of enzyme [56]. Then,
330 given the presence of genes encoding the complete classical pathway for glycogen
331 synthesis, it can be suggested that the glucan would act as a molecule for carbon and energy
332 storage in *Melainabacteria* [4], possibly with some structural particularities yet to be
333 elucidated [57].

334 The hypothesis of glycogen as a carbon/energy allocation molecule in
335 *Melainabacteria* is reinforced by the presence of the gene encoding the maltosyl-
336 transferase GlgE (EC 2.4.99.16), an enzyme that elongates a linear α -1,4-glucan in two
337 glucose units [58]. The latter was only characterized from actinobacterial sources, being
338 crystallized the one from *Streptomyces* [59] or proposed as an anti-tuberculosis drug [60].
339 The presence of genes for two glycogen pathways was postulated after *in silico* analysis
340 [61], demonstrated in *M. tuberculosis* [62,63], and very recently biochemically
341 characterized in *Chlamydia* [64]. Also, it was established that the mycobacterial GlgA
342 enzyme catalyzes the synthesis of maltose-1P, the specific substrate for glycogen
343 elongation by GlgE [65]. The substrates for maltose-1P synthesis by the mycobacterial
344 GlgA (now GlgM) are Glc-1P (acceptor) and ADP-Glc (glucosyl donor), both closely
345 linked to ADP-GlcPPase activity, thus strengthening the leading role of the latter in

346 bacterial glycogen metabolism. Altogether, the biochemical characterization of ADP-
347 GlcPPases from *Melainabacteria* and the analysis of genes co-existing in their genome
348 allowed us to postulate that carbon management in these bacteria is similar to that from
349 other heterotrophic microorganisms, particularly Actinobacteria. On the other hand, we
350 found no genes related to the synthesis of sucrose in *Melainabacteria* [e.g., sucrose-6P
351 synthase (EC 2.4.1.14) and sucrose synthase (EC 2.4.1.13)], as it occurs in *Anabaena* (see
352 Table 2). Thus, we hypothesize that this might be a critical difference between *Anabaena*
353 (and other cyanobacterial organisms) with the sister-clade *Melainabacteria*. This difference
354 might be reflected in the different regulatory properties of the respective ADP-GlcPPases.

355 Overall, the comparative analysis between ADP-GlcPPases from *Anabaena* PCC
356 7120 and *Melainabacteria* would help to discover new allosteric regulators in future
357 biochemical studies. This work emphasizes the importance of understanding the link
358 between the synthesis of storage compounds, like glycogen, with metabolites that indicate
359 the carbon and energy status of the cell, by studying the kinetic, regulatory, and structural
360 features of important metabolic enzymes. To the best of our knowledge, this is the first
361 biochemical report on enzymes involved in metabolic pathways from *Melainabacteria*,
362 adding data to the hot topic related to the separation of photosynthetic and non-
363 photosynthetic cyanobacteria.

364

365 **Acknowledgments**

366 This work was supported by grants from ANPCyT (PICT'17 1515 and PICT'18
367 00929 to AAI; PICT'18 00698 to MDAD and PICT'18 00865 to CMF), National Science
368 Foundation (grants MCB 1616851 to MAB) and CONICET (PUE-2016-0040 to IAL).
369 MVF is a Fellow from CONICET. RAH was a recipient of a Scholarship from Al Baha
370 University, Saudi Arabia. CMF, AAI and MDAD are Career Investigator members from
371 CONICET.

372 **Contribution**

373 CMF, MAB, AAI and MDAD designed the work; MVF, RH, MDAD data collection;
374 CMF, MAB, AAI and MDAD analyzed the data; MVF, CMF, MAB, AAI and MDAD
375 wrote the manuscript; all authors have approved the final article.

376

377

References

378

- 379 [1] M.A. Ballicora, A.A. Iglesias, J. Preiss, ADP-glucose pyrophosphorylase: a
380 regulatory enzyme for plant starch synthesis, *Photosynth. Res.* 79 (2004) 1–24.
381 <https://doi.org/10.1023/B:PRES.0000011916.67519.58>.
- 382 [2] M.A. Ballicora, A.A. Iglesias, J. Preiss, ADP-glucose pyrophosphorylase, a
383 regulatory enzyme for bacterial glycogen synthesis, *Microbiol. Mol. Biol. Rev.* 67
384 (2003) 213–225. <https://doi.org/10.1128/MMBR.67.2.213-225.2003>.
- 385 [3] A.A. Iglesias, J. Preiss, Bacterial glycogen and plant starch biosynthesis, *Biochem.*
386 *Educ.* 20 (1992) 196–203. [https://doi.org/10.1016/0307-4412\(92\)90191-N](https://doi.org/10.1016/0307-4412(92)90191-N).
- 387 [4] J. Preiss, Glycogen Biosynthesis, *Encycl. Microbiol. M. Echaech* (2009).
- 388 [5] M.A. Ballicora, J.I. Sesma, A.A. Iglesias, J. Preiss, Characterization of chimeric
389 ADP-glucose pyrophosphorylases of *Escherichia coli* and *Agrobacterium*
390 *tumefaciens*. Importance of the C-terminus on the selectivity for allosteric regulators,
391 *Biochemistry.* 41 (2002) 9431–9437. <https://doi.org/10.1021/bi025793b>.
- 392 [6] D.F. Gómez-Casati, R.Y. Igarashi, C.N. Berger, M.E. Brandt, A.A. Iglesias, C.R.
393 Meyer, Identification of functionally important amino-terminal Arginines of
394 *Agrobacterium tumefaciens* ADP-glucose pyrophosphorylase by alanine scanning
395 mutagenesis, *Biochemistry.* 40 (2001) 10169–10178.
396 <https://doi.org/10.1021/bi002615e>.
- 397 [7] M. Ballicora, E. Erben, T. Yazaki, ... A.B., Identification of regions critically
398 affecting kinetics and allosteric regulation of the *Escherichia coli* ADP-glucose
399 pyrophosphorylase by modeling and pentapeptide-scanning mutagenesis, *J.*
400 *Bacteriol.* 189 (2007) 5325–5333.
- 401 [8] M.D. Asención Diez, M.C. Aleanzi, A.A. Iglesias, M.A. Ballicora, A novel dual
402 allosteric activation mechanism of *Escherichia coli* ADP-glucose
403 pyrophosphorylase: The role of pyruvate, *PLoS One.* 9 (2014) e103888.
404 <https://doi.org/10.1371/journal.pone.0103888>.
- 405 [9] M.D. Asención Diez, C.M. Figueroa, M.C. Esper, R. Mascarenhas, M.C. Aleanzi, D.
406 Liu, M.A. Ballicora, A.A. Iglesias, On the simultaneous activation of *Agrobacterium*
407 *tumefaciens* ADP-glucose pyrophosphorylase by pyruvate and fructose 6-phosphate,
408 *Biochimie.* 171-172 (2020) 23–30. <https://doi.org/10.1016/j.biochi.2020.01.012>.
- 409 [10] D.F. Gómez Casati, M.A. Aon, A.A. Iglesias, Ultrasensitive glycogen synthesis in
410 Cyanobacteria, *FEBS Lett.* 446 (1999) 117–121. [https://doi.org/10.1016/S0014-5793\(99\)00201-X](https://doi.org/10.1016/S0014-5793(99)00201-X).
- 412 [11] A.A. Iglesias, G. Kakefuda, J. Preiss, Regulatory and structural properties of the
413 cyanobacterial ADP-glucose pyrophosphorylases, *Plant Physiol.* 97 (1991) 1187–
414 1195. <https://doi.org/https://doi.org/10.1104/pp.97.3.1187>.
- 415 [12] D.F. Gómez-Casati, S. Cortassa, M.A. Aon, A.A. Iglesias, Ultrasensitive behavior in
416 the synthesis of storage polysaccharides in cyanobacteria, *Planta.* 216 (2003) 969–
417 975. <https://doi.org/10.1007/s00425-002-0949-4>.
- 418 [13] B.A. Whitton, M. Potts, *The ecology of Cyanobacteria: their diversity in time and*
419 *space*, NY: KluwerAcademic Publishers, New York, 2002. <https://doi.org/doi:10.1007/0-306-46855-7>.
- 420

- 421 [14] W.W. Fischer, J. Hemp, J.S. Valentine, How did life survive Earth's great
422 oxygenation?, *Curr. Opin. Chem. Biol.* 31 (2016) 166–178.
423 <https://doi.org/10.1016/j.cbpa.2016.03.013>.
- 424 [15] R. Rippka, J. Deruelles, J.B. Waterbury, Generic assignments, strain histories and
425 properties of pure cultures of cyanobacteria, *J. Gen. Microbiol.* 111 (1979) 1–61.
426 <https://doi.org/10.1099/00221287-111-1-1>.
- 427 [16] J. Komárek, J. Kaštovský, J. Mareš, J.R. Johansen, Taxonomic classification of
428 cyanoprokaryotes (cyanobacterial genera) 2014, using a polyphasic approach,
429 *Preslia.* 86 (2014) 295–335.
- 430 [17] P.M. Shih, D. Wu, A. Latifi, S.D. Axen, D.P. Fewer, E. Talla, A. Calteau, F. Cai, N.
431 Tandeau De Marsac, R. Rippka, M. Herdman, K. Sivonen, T. Coursin, T. Laurent, L.
432 Goodwin, M. Nolan, K.W. Davenport, C.S. Han, E.M. Rubin, J.A. Eisen, T. Woyke,
433 M. Gugger, C.A. Kerfeld, Improving the coverage of the cyanobacterial phylum
434 using diversity-driven genome sequencing, *Proc. Natl. Acad. Sci. U. S. A.* 110
435 (2013) 1053–1058. <https://doi.org/10.1073/pnas.1217107110>.
- 436 [18] M.L. Sogin, H.G. Morrison, J.A. Huber, D.M. Welch, S.M. Huse, P.R. Neal, J.M.
437 Arrieta, G.J. Herndl, Microbial diversity in the deep sea and the underexplored “rare
438 biosphere,” *Proc. Natl. Acad. Sci. U. S. A.* 103 (2006) 12115–12120.
439 <https://doi.org/10.1073/pnas.0605127103>.
- 440 [19] S.C. Di Rienzi, I. Sharon, K.C. Wrighton, O. Koren, L.A. Hug, B.C. Thomas, J.K.
441 Goodrich, J.T. Bell, T.D. Spector, J.F. Banfield, R.E. Ley, The human gut and
442 groundwater harbor non-photosynthetic bacteria belonging to a new candidate
443 phylum sibling to Cyanobacteria, *Elife.* 2 (2013) e01102.
444 <https://doi.org/10.7554/eLife.01102.001>.
- 445 [20] R.M. Soo, C.T. Skennerton, Y. Sekiguchi, M. Imelfort, S.J. Paech, P.G. Dennis, J.A.
446 Steen, D.H. Parks, G.W. Tyson, P. Hugenholtz, An expanded genomic
447 representation of the phylum Cyanobacteria, *Genome Biol. Evol.* 6 (2014) 1031–
448 1045. <https://doi.org/10.1093/gbe/evu073>.
- 449 [21] K. Anantharaman, C.T. Brown, L.A. Hug, I. Sharon, C.J. Castelle, A.J. Probst, B.C.
450 Thomas, A. Singh, M.J. Wilkins, U. Karaoz, E.L. Brodie, K.H. Williams, S.S.
451 Hubbard, J.F. Banfield, Thousands of microbial genomes shed light on
452 interconnected biogeochemical processes in an aquifer system, *Nat. Commun.* 7
453 (2016) 13219. <https://doi.org/10.1038/ncomms13219>.
- 454 [22] R.M. Soo, J. Hemp, D.H. Parks, W.W. Fischer, P. Hugenholtz, On the origins of
455 oxygenic photosynthesis and aerobic respiration in Cyanobacteria, *Science* (80-.).
456 355 (2017) 1436–1440. <https://doi.org/10.1126/science.aal3794>.
- 457 [23] P.M. Shih, J. Hemp, L.M. Ward, N.J. Matzke, W.W. Fischer, Crown group
458 *Oxyphotobacteria* postdate the rise of oxygen, *Geobiology.* (2016) 1–11.
459 <https://doi.org/10.1111/gbi.12200>.
- 460 [24] W.W. Fischer, J. Hemp, J.E. Johnson, Evolution of Oxygenic Photosynthesis, *Annu.*
461 *Rev. Earth Planet. Sci.* 44 (2016) 647–683. <https://doi.org/10.1146/annurev-earth-060313-054810>.
- 462
463 [25] N. Salmaso, D. Albanese, C. Capelli, A. Boscaini, M. Pindo, C. Donati, Diversity
464 and cyclical seasonal transitions in the bacterial community in a large and deep
465 perialpine lake, *Microb. Ecol.* 76 (2018) 125–143. [20](https://doi.org/10.1007/s00248-</p></div><div data-bbox=)

- 466 017-1120-x.
- 467 [26] R.E. Ley, F. Bäckhed, P. Turnbaugh, C.A. Lozupone, R.D. Knight, J.I. Gordon,
468 Obesity alters gut microbial ecology, *Proc. Natl. Acad. Sci. U. S. A.* 102 (2005)
469 11070–11075. <https://doi.org/10.1073/pnas.0504978102>.
- 470 [27] A.A. Iglesias, M.A. Ballicora, J.I. Sesma, J. Preiss, Domain swapping between a
471 cyanobacterial and a plant subunit ADP-glucose pyrophosphorylase, *Plant Cell*
472 *Physiol.* 47 (2006) 523–530. <https://doi.org/10.1093/pcp/pcj021>.
- 473 [28] M.L. Kuhn, C.M. Figueroa, A.A. Iglesias, M.A. Ballicora, The ancestral activation
474 promiscuity of ADP-glucose pyrophosphorylases from oxygenic photosynthetic
475 organisms, *BMC Evol. Biol.* 13 (2013) 51. <https://doi.org/10.1186/1471-2148-13-51>.
- 476 [29] J. Sambrook, D. Russell, *Molecular cloning: a laboratory manual*, 3rd ed, Cold
477 Spring Harbor Laboratory Press, Cold Spring Harbor, NY, 2001.
- 478 [30] F. Jeanmougin, J.D. Thompson, M. Gouy, D.G. Higgins, T.J. Gibson, Multiple
479 sequence alignment with Clustal X, *Trends Biochem. Sci.* 23 (1998) 403–405.
480 [https://doi.org/10.1016/S0968-0004\(98\)01285-7](https://doi.org/10.1016/S0968-0004(98)01285-7).
- 481 [31] T.A. Hall, BioEdit: a user-friendly biological sequence alignment editor and analysis
482 program for Windows 95/98/NT, *Nucleic Acids Symp.* 41 (1999) 95–98.
- 483 [32] M. Gouy, S. Guindon, O. Gascuel, SeaView Version 4: a multiplatform graphical
484 user interface for sequence alignment and phylogenetic tree building, *Mol. Biol.*
485 *Evol.* 27 (2010) 221–224. <https://doi.org/10.1093/molbev/msp259>.
- 486 [33] M.M. Bradford, A rapid and sensitive method for the quantitation of microgram
487 quantities of protein utilizing the principle of protein-dye binding, *Anal. Biochem.*
488 72 (1976) 248–254.
- 489 [34] U.K. Laemmli, Cleavage of structural proteins during the assembly of the head of
490 bacteriophage T4, *Nature.* 227 (1970) 680–685.
- 491 [35] C. Fusari, A. Demonte, C. Figueroa, M. Aleanzi, A. Iglesias, A colorimetric method
492 for the assay of ADP-glucose pyrophosphorylase, *Anal. Biochem.* 352 (2006) 145–
493 147.
- 494 [36] M.A. Ballicora, E.D. Erben, T. Yazaki, A.L. Bertolo, A.M. Demonte, J.R. Schmidt,
495 M. Aleanzi, C.M. Bejar, C.M. Figueroa, C.M. Fusari, A.A. Iglesias, J. Preiss,
496 Identification of regions critically affecting kinetics and allosteric regulation of the
497 *Escherichia coli* ADP-glucose pyrophosphorylase by modeling and pentapeptide-
498 scanning mutagenesis, *J. Bacteriol.* 189 (2007) 5325–5333.
499 <https://doi.org/10.1128/JB.00481-07>.
- 500 [37] M.D. Asención Diez, S. Peirú, A.M. Demonte, H. Gramajo, A.A. Iglesias,
501 Characterization of recombinant UDP- and ADP-glucose pyrophosphorylases and
502 glycogen synthase to elucidate glucose-1-phosphate partitioning into oligo- and
503 polysaccharides in *Streptomyces coelicolor*, *J. Bacteriol.* 194 (2012) 1485–93.
504 <https://doi.org/10.1128/JB.06377-11>.
- 505 [38] M. Machtey, M.L. Kuhn, D.A. Flasch, M. Aleanzi, M.A. Ballicora, A.A. Iglesias,
506 Insights into glycogen metabolism in chemolithoautotrophic bacteria from
507 distinctive kinetic and regulatory properties of ADP-glucose pyrophosphorylase
508 from *Nitrosomonas europaea*, *J. Bacteriol.* 194 (2012) 6056–6065.
509 <https://doi.org/10.1128/JB.00810-12>.
- 510 [39] M.D. Asención Diez, A.M. Demonte, K. Syson, D.G. Arias, A. Gorelik, S.A.

- 511 Guerrero, S. Bornemann, A.A. Iglesias, Allosteric regulation of the partitioning of
512 glucose-1-phosphate between glycogen and trehalose biosynthesis in *Mycobacterium*
513 *tuberculosis*, *Biochim Biophys Acta.* 1850 (2015) 13–21.
514 <https://doi.org/10.1016/j.bbagen.2014.09.023>.
- 515 [40] D.F. Gómez Casati, M.A. Aon, A.A. Iglesias, Kinetic and structural analysis of the
516 ultrasensitive behaviour of cyanobacterial adp-glucose pyrophosphorylase, *Biochem.*
517 *J.* 350 (2000) 139–147. <https://doi.org/10.1042/0264-6021:3500139>.
- 518 [41] G. Kakefuda, Y.Y. Charng, A.A. Iglesias, L. McIntosh, J. Preiss, Molecular cloning
519 and sequencing of ADP-glucose pyrophosphorylase from *Synechocystis* PCC 6803,
520 *Plant Physiol.* 99 (1992) 359–361. <https://doi.org/10.1104/pp.99.1.359>.
- 521 [42] C.F. Demoulin, Y.J. Lara, L. Cornet, C. François, D. Baurain, A. Wilmotte, E.J.
522 Javaux, Cyanobacteria evolution: Insight from the fossil record, *Free Radic. Biol.*
523 *Med.* 140 (2019) 206–223. <https://doi.org/10.1016/j.freeradbiomed.2019.05.007>.
- 524 [43] J.A. Bhayani, B.L. Hill, A. Sharma, A.A. Iglesias, K.W. Olsen, M.A. Ballicora,
525 Mapping of a regulatory site of the *Escherichia coli* ADP-glucose
526 pyrophosphorylase, *Front. Mol. Biosci.* 6 (2019) 89–89.
527 <https://doi.org/10.3389/fmolb.2019.00089>.
- 528 [44] B.L. Hill, R. Mascarenhas, H.P. Patel, M.D. Asencion Diez, R. Wu, A.A. Iglesias, D.
529 Liu, M.A. Ballicora, Structural analysis reveals a pyruvate-binding activator site in
530 the *Agrobacterium tumefaciens* ADP-glucose pyrophosphorylase, *J. Biol. Chem.* 294
531 (2019) 1338–1348. <https://doi.org/10.1074/jbc.RA118.004246>.
- 532 [45] B.L. Hill, J. Wong, B.M. May, F.B. Huerta, T.E. Manley, P.R.F. Sullivan, K.W.
533 Olsen, M.A. Ballicora, Conserved residues of the Pro103-Arg115 loop are involved
534 in triggering the allosteric response of the *Escherichia coli* ADP-glucose
535 pyrophosphorylase, *Protein Sci.* 24 (2015) 714–728.
536 <https://doi.org/10.1002/pro.2644>.
- 537 [46] C.M. Figueroa, M.C. Esper, A. Bertolo, A.M. Demonte, M. Aleanzi, A.A. Iglesias,
538 M.A. Ballicora, Understanding the allosteric trigger for the fructose-1,6-
539 bisphosphate regulation of the ADP-glucose pyrophosphorylase from *Escherichia*
540 *coli*, *Biochimie.* 93 (2011) 1816–1823. <https://doi.org/10.1016/j.biochi.2011.06.029>.
- 541 [47] A.E. Cereijo, M.D. Asención Diez, M.A. Ballicora, A.A. Iglesias, Regulatory
542 properties of the ADP-glucose pyrophosphorylase from the Clostridial *Firmicutes*
543 member *Ruminococcus albus*, *J. Bacteriol.* 200 (2018) e00172–18.
- 544 [48] M.D. Asención Diez, A.M. Demonte, S.A. Guerrero, M.A. Ballicora, A.A. Iglesias,
545 The ADP-glucose pyrophosphorylase from *Streptococcus mutans* provides evidence
546 for the regulation of polysaccharide biosynthesis in Firmicutes, *Mol. Microbiol.* 90
547 (2013) 1011–1027. <https://doi.org/10.1111/mmi.12413>.
- 548 [49] J. Preiss, Bacterial glycogen inclusions: enzymology and regulation of synthesis, in:
549 *Inclusions in Prokaryotes*, Springer-Verlag, 2006: pp. 71–108.
550 https://doi.org/10.1007/3-540-33774-1_4.
- 551 [50] A.E. Cereijo, M.D. Asención Diez, J.S. Dávila Costa, H.M. Alvarez, A.A. Iglesias,
552 On the kinetic and allosteric regulatory properties of the ADP-glucose
553 pyrophosphorylase from *Rhodococcus jostii*: An approach to evaluate glycogen
554 metabolism in oleaginous bacteria, *Front. Microbiol.* 7 (2016) 830.
555 <https://doi.org/10.3389/fmicb.2016.00830>.

- 556 [51] A.E. Cereijo, H.M. Alvarez, A.A. Iglesias, M.D. Asención Díez, Glucosamine-P and
557 rhodococcal ADP-glucose pyrophosphorylases: A hint to (re)discover
558 (actino)bacterial amino sugar metabolism, *Biochimie*. 176 (2020) 158–161.
559 <https://doi.org/10.1016/j.biochi.2020.07.006>.
- 560 [52] D. Kadouche, M. Ducatez, U. Cenci, C. Tirtiaux, E. Suzuki, Y. Nakamura, J.-L.
561 Putaux, D. Terrasson, S. Diaz-Troya, F.J. Florencio, M.C. Arias, A. Striebeck, M.
562 Palcic, S.G. Ball, C. Colleoni, Characterization of function of the GlgA2
563 glycogen/starch synthase in *Cyanobacterium* sp. Clg1 highlights convergent
564 evolution of glycogen metabolism into starch granule aggregation, *Plant Physiol*.
565 171 (2016) 1879–1892. <https://doi.org/10.1104/pp.16.00049>.
- 566 [53] K. Syson, C.E.M. Stevenson, D.M. Lawson, S. Bornemann, Structure of the
567 *Mycobacterium smegmatis* α -maltose-1-phosphate synthase GlgM, *Acta Crystallogr.*
568 *Sect. F Struct. Biol. Commun.* 76 (2020) 175–181.
569 <https://doi.org/10.1107/S2053230X20004343>.
- 570 [54] V. Lombard, H. Golaconda Ramulu, E. Drula, P.M. Coutinho, B. Henrissat, The
571 carbohydrate-active enzymes database (CAZy) in 2013, *Nucleic Acids Res.* 42
572 (2014) D490–D495. <https://doi.org/10.1093/nar/gkt1178>.
- 573 [55] M. Palomo, T. Pijning, T. Booiman, J.M. Dobruchowska, J. Van Der Vlist, S. Kralj,
574 A. Planas, K. Loos, J.P. Kamerling, B.W. Dijkstra, M.J.E.C. Van Der Maarel, L.
575 Dijkhuizen, H. Leemhuis, *Thermus thermophilus* glycoside hydrolase family 57
576 branching enzyme: Crystal structure, mechanism of action, and products formed, *J.*
577 *Biol. Chem.* 286 (2011) 3520–3530. <https://doi.org/10.1074/jbc.M110.179515>.
- 578 [56] X. Zhang, H. Leemhuis, M.J.E.C. Van Der Maarel, Characterization of the GH13
579 and GH57 glycogen branching enzymes from *Petrotoga mobilis* SJ95 and potential
580 role in glycogen biosynthesis, *PLoS One*. 14 (2019) e0219844.
581 <https://doi.org/10.1371/journal.pone.0219844>.
- 582 [57] M. Colpaert, M. Chabi, U. Cenci, C. Colleoni, Storage Polysaccharides in
583 Prokaryotes: Glycogen, Granulose, and Starch-Like Granules, in: 2020: pp. 177–
584 210. https://doi.org/10.1007/978-3-030-60173-7_8.
- 585 [58] A.D. Elbein, I. Pastuszak, A.J. Tackett, T. Wilson, Y.T. Pan, Last step in the
586 conversion of trehalose to glycogen. A mycobacterial enzyme that transfers maltose
587 from maltose 1-phosphate to glycogen, *J. Biol. Chem.* 285 (2010) 9803–9812.
588 <https://doi.org/10.1074/jbc.M109.033944>.
- 589 [59] K. Syson, C.E.M. Stevenson, M. Rejzek, S.A. Fairhurst, A. Nair, C.J. Bruton, R.A.
590 Field, K.F. Chater, D.M. Lawson, S. Bornemann, Structure of *Streptomyces*
591 maltosyltransferase GlgE, a homologue of a genetically validated anti-tuberculosis
592 target, *J. Biol. Chem.* 286 (2011) 38298–38310.
593 <https://doi.org/10.1074/jbc.M111.279315>.
- 594 [60] R. Kalscheuer, K. Syson, U. Veeraghavan, B. Weinrick, K.E. Biermann, Z. Liu,
595 J.C. Sacchettini, G. Besra, S. Bornemann, W.R. Jacobs, Self-poisoning of
596 *Mycobacterium tuberculosis* by targeting GlgE in an α -glucan pathway, *Nat. Chem.*
597 *Biol.* 6 (2010) 376–384. <https://doi.org/10.1038/nchembio.340>.
- 598 [61] G. Chandra, K.F. Chater, S. Bornemann, Unexpected and widespread connections
599 between bacterial glycogen and trehalose metabolism, *Microbiology*. 157 (2011)
600 1565–1572. <https://doi.org/10.1099/mic.0.044263-0>.

- 601 [62] T. Sambou, P. Dinadayala, G. Stadthagen, N. Barilone, Y. Bordat, P. Constant, F.
602 Levillain, O. Neyrolles, B. Gicquel, A. Lemassu, M. Daffé, M. Jackson, Capsular
603 glucan and intracellular glycogen of *Mycobacterium tuberculosis*: Biosynthesis and
604 impact on the persistence in mice, *Mol. Microbiol.* 70 (2008) 762–774.
605 <https://doi.org/10.1111/j.1365-2958.2008.06445.x>.
- 606 [63] R. Kalscheuer, W.R. Jacobs, The significance of GlgE as a new target for
607 tuberculosis, *Drug News Perspect.* 23 (2010) 619–624.
608 <https://doi.org/10.1358/dnp.2010.23.10.1534855>.
- 609 [64] M. Colpaert, D. Kadouche, M. Ducatez, T. Pillonel, C. Kebbi-Beghdadi, U. Cenci,
610 B. Huang, M. Chabi, E. Maes, B. Coddeville, L. Couderc, H. Touzet, F. Bray, C.
611 Tirtiaux, S. Ball, G. Greub, C. Colleoni, Conservation of the glycogen metabolism
612 pathway underlines a pivotal function of storage polysaccharides in Chlamydiae,
613 *Commun. Biol.* 4 (2021) 296. <https://doi.org/10.1038/s42003-021-01794-y>.
- 614 [65] H. Koliwer-Brandl, K. Syson, R. van de Weerd, G. Chandra, B. Appelmelk, M.
615 Alber, T.R. Ioerger, W.R. Jacobs, J. Geurtsen, S. Bornemann, R. Kalscheuer,
616 Metabolic network for the biosynthesis of intra- and extracellular α -glucans required
617 for virulence of *Mycobacterium tuberculosis*, *PLOS Pathog.* 12 (2016) e1005768.
618 <https://doi.org/10.1371/journal.ppat.1005768>.

619

620

621

622 **Figure legends**

623 **Figure 1. Phylogenetic tree of GlgC from different organisms.** The tree was built as
624 described in Materials and Methods. Protein sequences are numbered with codes indexed in
625 Supplemental Table S3.

626 **Figure 2. Effect of different metabolites on the activity of ADP-GlcPPases from non-**
627 **photosynthetic cyanobacteria. (A)** Intestinal *Melainabacteria* GlgC and **(B)** free-living
628 *Melainabacteria* GlgC. Relative activities were calculated as the ratio between the activities
629 in the presence and absence of the respective effector. The value of 1 corresponds to the
630 respective ADP-GlcPPase V_{\max} (see Table 1). The metabolite concentration was 2.5 mM in
631 all cases. Assays were performed using two sets of Glc-1P and ATP concentrations:
632 subsaturating (dark gray bars) or saturating (light gray bars).

633 **Figure 3. Activation of cyanobacterial ADP-GlcPPases by Glc-6P (A) and 3-PGA (B).**
634 Intestinal *Melainabacteria* GlgC (filled circles), free-living *Melainabacteria* GlgC (filled
635 squares), *Anabaena* GlgC (filled triangle). The value of 1 corresponds to activities of 7.0,
636 2.0, and 0.25 U/mg for in*Mel*GlgC, fl*Mel*GlgC, and *Anabaena* ADP-GlcPPases,
637 respectively.

638

639 **Table 1.** Kinetic parameters for the cyanobacterial ADP-GlcPPases characterized in this
 640 work in the absence and in the presence of allosteric activators. Activity was assayed as
 641 described in Materials and Methods. Kinetic parameters were calculated by the fitting
 642 software, using the mean of three independent datasets.

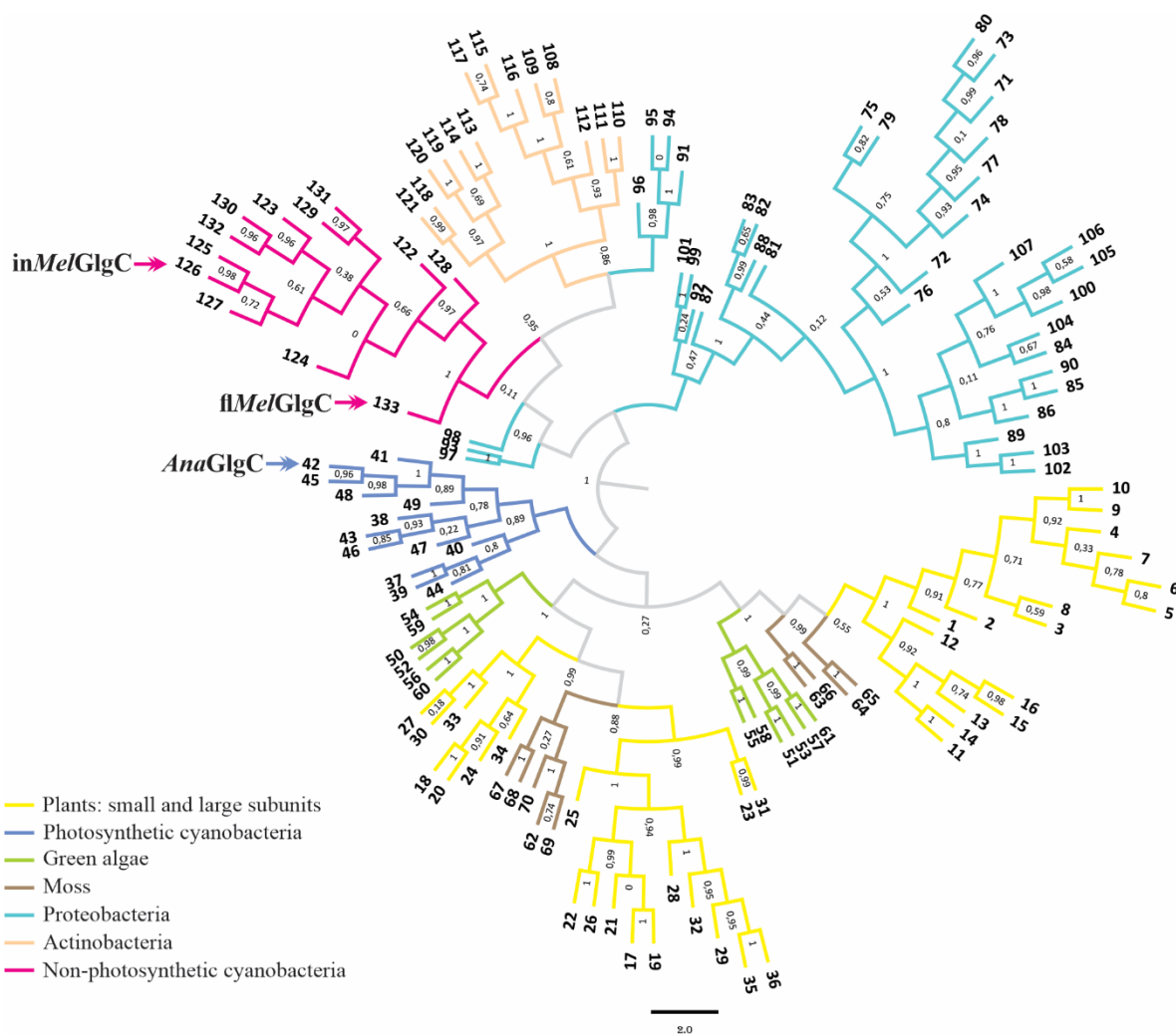
| Effector and Parameter | <i>inMelGlgC</i> | | <i>f1MelGlgC</i> | | <i>AnaGlgC</i> | |
|------------------------------|------------------|-------------------|------------------|-----------------|-----------------|-----------------|
| | Glc-1P | ATP | Glc-1P | ATP | Glc-1P | ATP |
| <i>None</i> | | | | | | |
| $S_{0.5}$ (mM) | 0.32 ± 0.03 | 0.25 ± 0.01 | 2.1 ± 0.2 | 0.34 ± 0.05 | 0.08 ± 0.02 | 0.40 ± 0.04 |
| n_H | 1.3 | 1.8 | 1.6 | 1.4 | 0.7 | 1.2 |
| V_{max} (U/mg) | 6.7 ± 0.2 | 7.1 ± 0.1 | 2.3 ± 0.1 | 1.9 ± 0.1 | 0.20 ± 0.01 | 0.31 ± 0.01 |
| <i>Glc-6P</i> | | | | | | |
| $S_{0.5}$ (mM) | 0.20 ± 0.02 | 0.18 ± 0.01 | 0.55 ± 0.02 | 0.5 ± 0.1 | 0.9 ± 0.4 | 0.55 ± 0.08 |
| n_H | 1.2 | 1.6 | 1.9 | 1 | 0.6 | 2.5 |
| V_{max} (U/mg) | 366 ± 10 | 444 ± 8 | 12.4 ± 0.2 | 14.7 ± 0.8 | 1.6 ± 0.2 | 1.30 ± 0.09 |
| <i>Fru-6P</i> | | | | | | |
| $S_{0.5}$ (mM) | 0.09 ± 0.01 | 0.151 ± 0.005 | 0.9 ± 0.2 | 0.3 ± 0.1 | 0.3 ± 0.1 | 0.40 ± 0.04 |
| n_H | 1.1 | 1.6 | 0.8 | 1 | 0.8 | 1.2 |
| V_{max} (U/mg) | 317 ± 10 | 357 ± 5 | 6.4 ± 0.5 | 8.3 ± 0.8 | 1 ± 0.01 | 0.31 ± 0.01 |

643

644 **Table 2.** Proteins detected after BLAST with data from *Melainabacteria*, compared to
 645 *Anabaena*.

| Gene | Intestinal <i>Melainabacteria</i> MELA1 | Free-living <i>Melainabacteria</i> GWF2_37_15 | <i>Anabaena</i> PCC 7120 |
|--------------|---|---|----------------------------------|
| <i>glgC</i> | ID: AOR37842.1 | ID: OGI00355.1 | ID: BAB76344.1 |
| <i>glgA</i> | ID: AOR37764.1 | ID: OGI01396.1 | ID: BAB73578.1 ID: BAB77555.1 |
| <i>glgB</i> | ID: AOR39099.1 | ID: OGI01242.1 | ID: BAB72670.1 |
| <i>glgX</i> | ID: AOR37731.1 | ID: OGI01270.1 | ID: BAB77692.1 |
| <i>glgP</i> | ID: AOR37860.1 | ID: OGI02531.1 | ID: BAB73229.1 |
| <i>glgE1</i> | ID: AOR39243.1 | ID: OGI01701.1 ID: OGI04937.1 | not found |
| <i>glgE2</i> | ID: AOR39243.1 | ID: OGI01701.1 ID: OGI04937.1 | not found |
| <i>sus</i> | not found | not found | ID: BAB76684.1 |
| <i>sps</i> | not found | not found | ID: BAB75069.1 ID: BAB72334.1 |

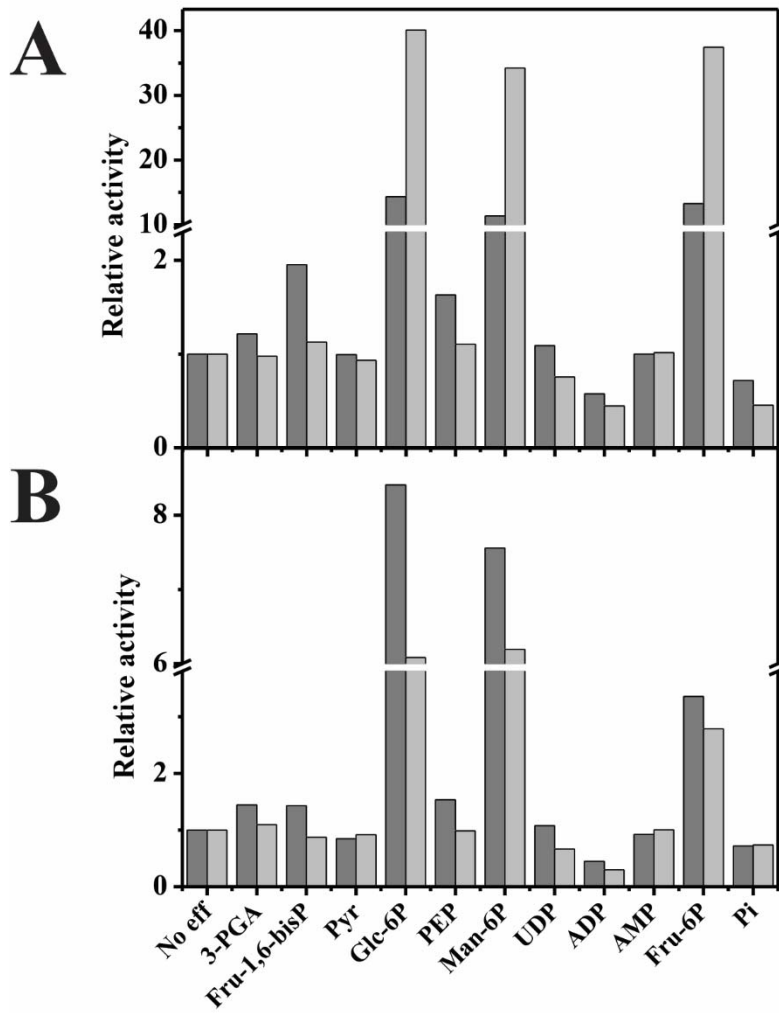
646 **Figure 1**



647

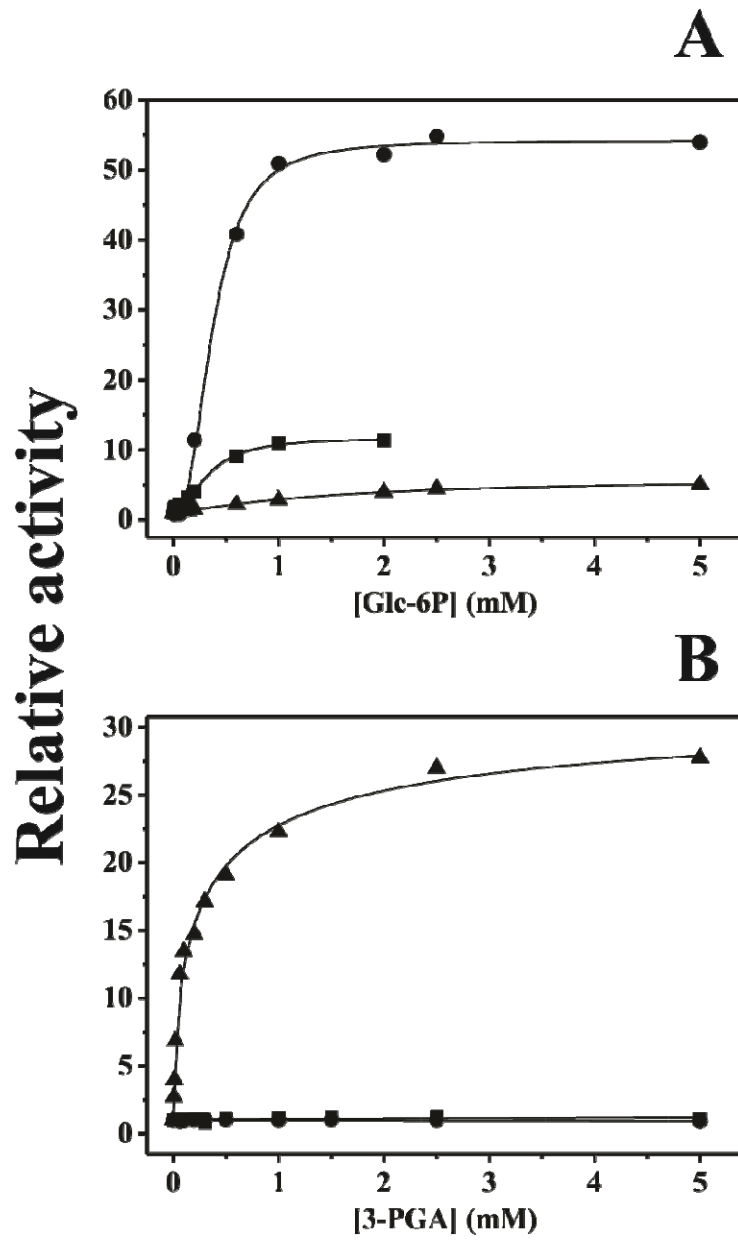
648

649 **Figure 2**



650

651 **Figure 3**



652